Kinetics and Reaction Mechanism of Hydroxyl Radical Reaction with Methyl Formate

David A. Good, Jaron Hanson, and Joseph S. Francisco*

Department of Chemistry and Department of Earth and Atmospheric Sciences, Purdue University, West Lafayette, Indiana 47907

Zhuangjie Li* and Gill-Ran Jeong

Department of Atmospheric Sciences, University of Illinois at Urbana-Champaign, Urbana, Illinois 61801

Received: June 14, 1999; In Final Form: September 24, 1999

Ab initio molecular orbital theory has been used to examine the kinetics and mechanism for the reaction of hydroxyl radical with methyl formate. From the *ab initio* parameters the room temperature rate constant is calculated and found to be in good agreement with the experimental determination. It is found that 86% of the reaction proceeds via abstraction of the carbonyl hydrogen from methyl formate by hydroxyl radical, resulting in the formation of CH_3OCO radical. CH_3OCO is expected to oxidize to formaldehyde and carbon dioxide under tropospheric conditions.

I. Introduction

Concerns about mobile source emissions and their impact on urban tropospheric ozone formation have spurred research into alternative fuels.[1−7] Fuel composition affects the tendency of a fuel to form soot particulates and NO_x. Increasing the carbon-to-hydrogen ratio or the number of carbon−carbon bonds increases the tendency of a fuel to form soot during combustion.[1] Oxygenated hydrocarbons such as ethers can be added to fuels to maintain performance while lowering tailpipe emissions of CO. Dimethyl ether (DME) is a fuel antiknock agent and proposed diesel fuel substitute. DME has been used as a methanol ignition improver in diesel engines where it has been reported to reduce hydrocarbon emissions. Some of its attractive features include low self-ignition temperature, low octane number (high cetane number, 55−60), and reduced combustion noise, particle emission, and NO_x emissions. DME-fueled engines are nonsooting and DME can be economically produced from a one-step synthesis. Engine tests have shown that DME-fueled diesel engines have emission levels that surpass the California Ultra Low Emissions Vehicle regulation for medium-duty vehicles.[1]

The oxidation of DME has been studied by Japar et al.,[2] Jenkin et al.,[3] Wallington et al.,[4] Langer et al.,[5] and Sehested et al.[6,7] Japar et al.[2] used $Cl^•$ atom and $OH^•$ radical initiated hydrogen abstraction to simulate the reaction of DME with tropospheric OH radical in the presence of NO. Reaction products were determined using FTIR spectroscopy. The production of methyl formate accompanied the loss of dimethyl ether quantitatively. The yield of methyl formate relative to DME loss was found to be 0.90.[2] The following reaction mechanism was put forth to rationalize experimental findings of methyl formate degradation initiated by chlorine atoms. The Cl atom initiates the hydrogen abstraction reaction, producing methoxy methyl radical, CH_2OCH_3. The addition of O_2 results in the formation of the methoxy methyl peroxyl radical, $O_2CH_2OCH_3$. The formed peroxyl radical relinquishes an oxygen atom to NO, forming NO_2 and the methoxy methoxyl radical OCH_2OCH_3. The final step involves hydrogen abstraction by O_2 to form methyl formate, $CH_3OC(O)H$, and HO_2. Hydrogen abstraction is found to occur at the CH_2 group. The other possibility would be O_2 attack at the H atom in the CH_3 group, forming OCH_2OCH_2 and ultimately two CH_2O molecules. However, no evidence of participation in this degradation channel was found.[2] Under atmospheric conditions dimethyl ether reacts almost quantitatively to form methyl formate.

Methyl formate can further participate in hydrogen abstraction reactions as mediated by tropospheric hydroxyl radical. Using a flash photolysis−resonance fluorescence technique, Wallington et al.[8] measured the 296 K rate constant of this reaction to be $(2.27 \pm 0.34) \times 10^{-13}$ cm^3 molecule^{-1} s^{-1}. Le Calve' et al.,[9] using a laser photolysis−laser-induced fluorescence technique, measured the temperature-dependent rate constant for OH attack on $CH_3OC(O)H$ to be $(8.54 \pm 1.98) \times 10^{-13} \exp[-(461 \pm 70)/T]$. The 298 K rate constant is calculated to be $(1.73 \pm 0.21) \times 10^{-13}$ cm^3 molecule^{-1} s^{-1}.[9] Using this data an estimate for the atmospheric lifetime of methyl formate with respect to loss from the OH radical reaction is 51−67 days. With a short lifetime of 67 days methyl formate is likely to decay predominantly in the troposphere. However, to the best of our knowledge no work has attempted to determine the products of the reaction between the hydroxyl radical and methyl formate. Hydrogen abstraction of methyl formate can occur at two distinct sites. The OH radical can remove a methyl hydrogen to form the $CH_2OC(O)H$ radical or the OH radical can remove the carbonyl hydrogen to from the CH_3OCO radical.

$$CH_3OC(O)H + OH \rightarrow CH_2OC(O)H + H_2O \quad (1a)$$

$$CH_3OC(O)H + OH \rightarrow CH_3OCO + H_2O \quad (1b)$$

It is a goal of this work to determine the relative importance of these two competing reaction channels in addition to verifying the above 298 K rate constant measurements using a discharge flow combined with a resonance fluorescence and mass spectrometer (DF/RF/MS) technique.

II. Methods

a. Computational. All calculations were performed with the Gaussian 94 package of programs.[10] Geometry optimizations

10.1021/jp991960e CCC: $18.00
Published on Web 11/09/1999

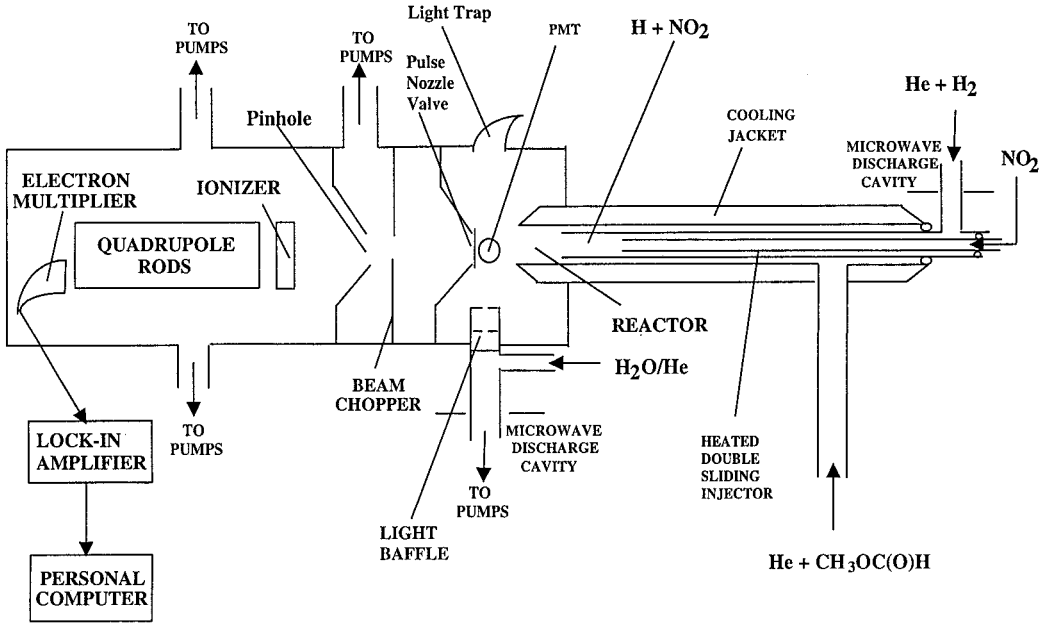

Figure 1. DF/MS/RF experimental apparatus for the study of OH + methyl formate.

for all species were carried out for all structures to better than 0.001 Å for bond lengths and 0.1° for angles. The geometries were fully optimized and with these geometries a frequency calculation was performed, all at the second-order Møller-Plesset (UMP2) level with the 6-31G(d) basis set. Restricted wave functions were used for closed-shell and unrestricted for open-shell systems with all orbitals active. In addition, G2 energies were calculated using G2 methodology.[11−13] The total energies are corrected to 0 K by adding the zero-point energy to the predicted total energy. To obtain the energy at 298 K, the thermal energy of each species is added to its total energy instead of the zero-point energy.

b. Experimental. The DF/RF/MS instrument used in this experiment is illustrated in Figure 1. Note that the drawing only illustrates the relative position of the instrument, not the actual size or distance of the instrumental elements. The DF/MS and DF/RF/MS systems in the present study have been described previously and are only briefly discussed here.[14,15] The reactor consisted of an 80-cm-long, 5.08-cm-i.d. Pyrex tube coated with halocarbon wax to reduce OH wall losses. The vacuum chamber for the discharge flow-modulated molecular beam mass spectrometer was a two-stage differentially pumped vacuum system utilizing two 6-in. diffusion pumps with liquid nitrogen baffles. The vacuum in the second stage was $<5 \times 10^{-10}$ Torr. A 125-cfm mechanical pump (Edwards Model E2M175) maintained the steady-state pressure in the reactor at normally 1 Torr. Helium was used as the main buffer gas and was admitted through a side arm located upstream of the reactor. The resulting reactor flow velocities ranged between 800 and 2000 cm s^{-1}; the corresponding gaseous residence times within the reactor were between 100 and 40 ms.

OH radicals were produced by reaction of H with NO_2.[12]

$$H + NO_2 \rightarrow OH + NO \qquad k_2 = 1.3 \times 10^{-10}\ \text{cm}^3\ \text{molecule}^{-1}\ \text{s}^{-1} \quad (2)$$

Atomic hydrogen was produced by the microwave discharge of H_2 and the OH radicals were detected by resonance fluorescence.[16−19] The resonance lamp used for the excitation of the $A^2\Sigma \rightarrow X^2\Pi$ transition in OH at 309 nm was built by a microwave discharging ~3 Torr of a H_2O/He mixture in a quartz tube.[18,20,21] The OH resonance fluorescence signal was monitored using a photomultiplier tube (HAMAMATSU HC124-02 with a R269 photomultiplier tube assembly) that was positioned perpendicular to the source radiation. A UV-enhanced spherical mirror ($l/f = 50$ mm, Edmund Scientific Co.) was placed in the OH fluorescence zone in alignment with the photomultiplier tube to increase the OH fluorescence photon collection. The OH fluorescence signals were sent to a lock-in amplifier (Model SR510, Stanford Research Systems, Inc.) that was referenced to a chopper frequency chopping the resonance radiation, and the signals were then digitized (Analog Devices RTI/815) and recorded on a microcomputer. Light baffles were placed in both pathways of resonance and fluorescence radiation to reduce the scattered light. It was found that the scattered light was greatly attenuated with the use of the light baffles. The proportionality constant relating the fluorescence signal to OH concentration was determined by titration of OH by Br_2 such that [OH] = [Br_2] consumed.

$$OH + Br_2 \rightarrow HOBr + Br \qquad k_3 = 4.2 \times 10^{-11}\ \text{cm}^3\ \text{molecule}^{-1}\ \text{s}^{-1} \quad (3)$$

Methyl formate was purchased from Aldrich, Inc. with a manufacture's stated purity of 99.9%. Samples of methyl formate were subjected to several freeze−pump−thaw cycles prior to use. The total rate constant ($k_1 = k_{1a} + k_{1b}$) was then measured. A general procedure of acquiring DF/MS and DF/RF/MS kinetic information for reactions involving radical species has been described previously.[22] Briefly, the pseudo-first-order ([methyl formate]$_0 \gg$ [OH]$_0$) rate constant for reaction 1 is given as

$$k'' = -v\ \text{d}(\ln[\text{OH}])/\text{d}z \quad (4)$$

where v is the carrier gas flow velocity and z is the injector position. k'' is further corrected using eq 5 where D is the diffusion coefficient of OH in helium and k_p is the decay rate of the OH radical due to both wall loss and OH self reaction.

$$k' = k''(1 + Dk''/v^2) - k_p \quad (5)$$

By variation of the initial methyl formate (MEF) concentration, different decay rates were collected. When the pseudo-first-order decay rate is plotted as a function of $[MEF]_0$, the slope of the fitted straight line yields the binary rate constant for reaction 1.

III. Results and Discussions

A. Geometry and Vibrational Frequencies. The structure of methyl formate, the radical products, and the two transition states as calculated at the MP2/6-31G(d) level of theory are illustrated in Figure 2. Methyl formate has C_s symmetry adopting a planar cis conformation as the lowest energy conformation, i.e., the C′OCO′ dihedral is 0.0°. The CH bond lengths in the methyl group are predicted to be 1.087, 1.090, and 1.090 Å. The CO bond adjacent to the methyl group was calculated to be 1.442 Å and the opposing CO single bond to be 1.345 Å. The C═O bond length in methyl formate was computed to be 1.214 Å. The carbonyl CH bond is predicted to be slightly longer than CH bonds in the methyl group having a CH bond length of 1.097 Å. The computed structure of methyl formate is in excellent agreement with the experimentally determined structure as given by Curl.[23] His work reports C−O single bonds of 1.437 and 1.334 Å and a C═O bond of 1.200 Å. The in-plane CH bond on the methyl group is reported to be 1.086 Å while the in-plane CH bond on the carbonyl group is determined to be 1.101 Å in length. Our calculated structural parameters deviate from the experimentally determined structural parameters by about 1%.

Hydrogen abstraction from methyl formate yields the CH_3OCO radical. As illustrated in Figure 2, the radical remains in C_s symmetry with dihedrals of HC′OC = 180.0° and C′OCO′ = 0.0°. Calculation at the MP2/6-31G(d) level suggests that the main structural changes incurred include a lengthening of the ether linkage C′O bond from 1.442 to 1.457 Å and a shortening of the opposing CO bond from 1.345 to 1.328 Å. The carbonyl CO′ bond also decreases to 1.201 Å. This pattern of increasing/decreasing CO bond lengths suggests that bond cleavage is more likely to form CO_2 and CH_3 as opposed to CH_3O and CO.

Hydrogen abstraction of methyl formate can also result in the formation of $CH_2OC(O)H$. The optimized configuration of $CH_2OC(O)H$ suggests that the remaining methyl hydrogens are in slightly out-of-plane positions. As shown in Figure 2, the calculated CH bonds of the CH_2 group are slightly shorter than the CH bond lengths found in methyl formate. The CO bond adjacent to the carbonyl group slightly increases in length compared to that of $CH_3OC(O)H$. The opposing C′O bond is predicted to decrease in length from 1.442 Å in methyl formate to 1.384 Å in $CH_2OC(O)H$.

Figure 2d illustrates the transition state in which the hydroxyl radical attacks one of the methyl hydrogens to form CH_2OCOH and H_2O. As mentioned, the hydroxyl radical prefers to attack one of the longer out-of-plane hydrogens rather than the shorter in-plane hydrogen. The breaking CH bond elongates to 1.218 Å while the forming OH bond shortens to 1.286 Å. Compared to $CH_3OC(O)H$, the C′O bond adjacent to the methyl group decreases by 0.025 Å while the opposing CO single bond increases by 0.014 Å in length.

Figure 2e illustrates the structure of the transition state in which the hydroxyl radical attacks the carbonyl hydrogen to form CH_3OCO and H_2O. The breaking CH bond is predicted to be 1.223 Å and the forming OH bond to be 1.291 Å in length. Compared to that of $CH_3OC(O)H$, the CO bond adjacent to the carbonyl group decreases while the CO bond adjacent to the methyl group slightly increases. In both transition states the C═O bond undergoes very little change in both length and position.

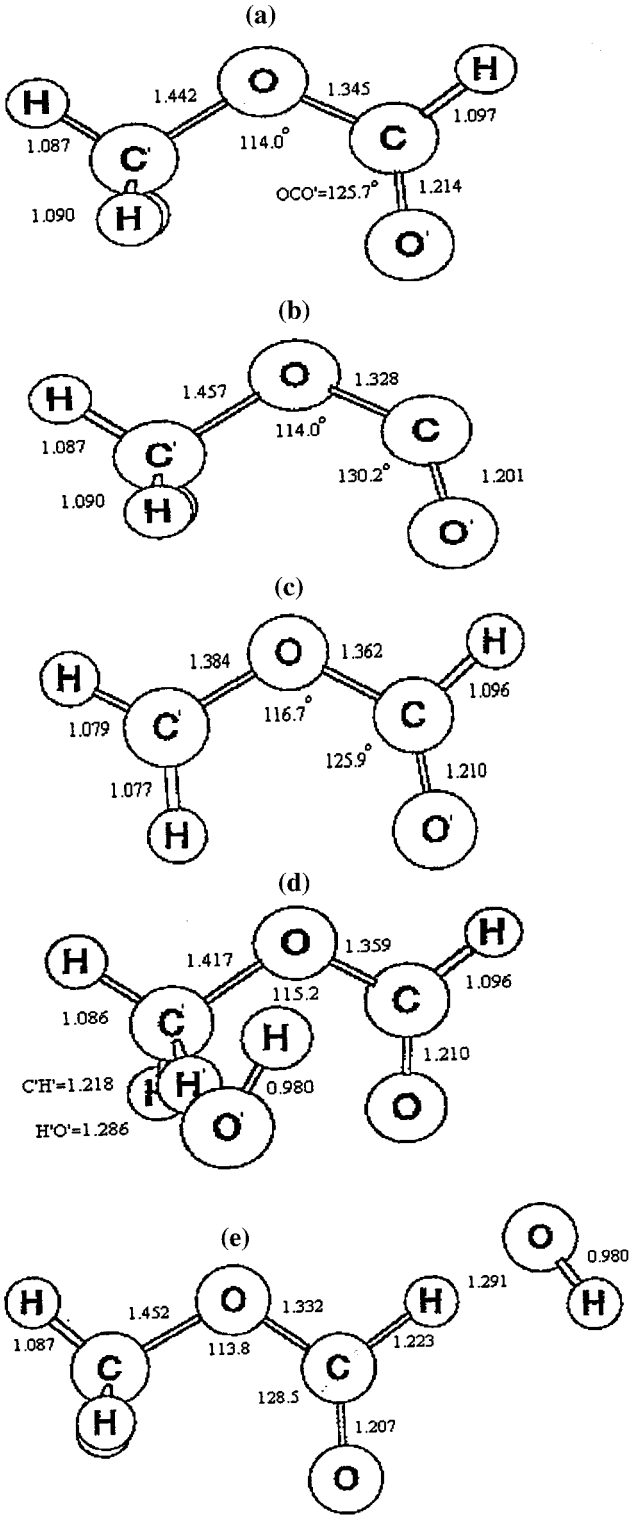

Figure 2. Calculated structures for species involved in reaction 1. The calculations were performed at the MP2/6-31G(d) level of theory. (a) structure of methyl formate; (b) structure of CH_3OCO radical; (c) structure of $CH_2OC(O)H$ radical; (d) structure of HO−$CH_3OC(O)H$ transition state; (e) structure of $CH_3OC(O)H$−OH transition state.

Table 1 lists the vibrational frequencies for methyl formate, alkyl radicals, and transition states. Also listed are the experimentally measured vibrational frequencies as reported by Shimanouchi for methyl formate.[25] Vibrational frequencies for

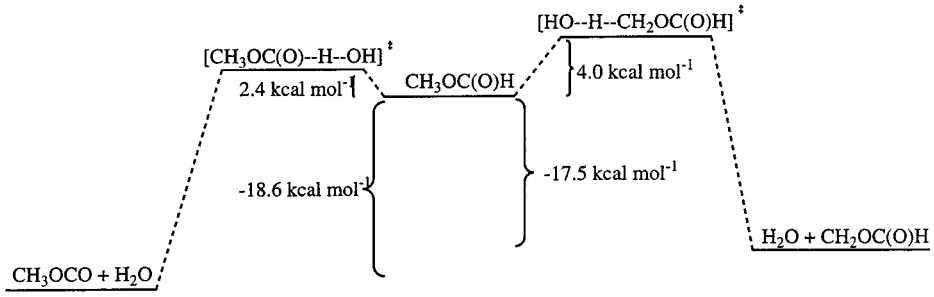

Figure 3. Comparison of methyl formate reaction pathways.

TABLE 1: Vibrational Frequencies Calculated at MP2/6-3 1 G(d) Level of Theory for Methyl Formate, Alkyl Radicals, and Transition States[a]

methyl formate	experimental[b]	CH_3OCO	$CH_2OC(O)H$	OH−$CH_3OC(O)H$	$CH_3OC(O)H$−OH
3102	3045	3111	3247	3541	3534
3069	3012	3076	3098	3127	3113
2988	2969	2979	3008	3022	3080
2978	2943	1774	1734	3000	2983
1728	1754	1476	1424	1735	1477
1481	1454	1473	1366	1489	1473
1474	1445	1433	1214	1433	1468
1442	1443	1169	1148	1361	1457
1362	1371	1133	980	1293	1434
1208	1207	1132	978	1205	1201
1158	1168	901	723	1161	1158
1150	1166	725	582	1107	1140
998	1032	371	333	989	1047
920	925	273	322	954	908
742	767	132	212	822	833
334	332			735	753
296	318			682	534
149	130			322	297
				319	286
				273	146
				98	136
				74	95
				45	73
				2294i	2505i

[a] All values in cm^{-1}. [b] From ref 25.

$CH_3OC(O)H$ as computed at the MP2/6-31G(d) level of theory have been shown to be systematically overestimated. Thus, the values listed in Table 1 have been scaled by 0.95 as recommended.[24] Our scaled values are in good agreement with the literature values for methyl formate with a deviation on the order of 2%. As shown in Table 1, both transition states have relatively large imaginary frequencies, suggesting a narrow passage through the transition state. Thus, tunneling will have a large effect on the rate constant of the hydrogen abstraction reaction.

B. Relative Energetics. The salient energetic parameters for each reactant and transition state are tabulated and illustrated in Table 2 and Figure 3. Removal of the carbonyl hydrogen is predicted to be favored both thermodynamically and kinetically. The reaction enthalpy for the removal of a methyl hydrogen (reaction 1a) is calculated to be exothermic by −17.5 kcal mol^{-1} while the removal of the carbonyl hydrogen (reaction 1b) is slightly more favorable, having a reaction enthalpy of −18.6 kcal mol^{-1}. Removal of the carbonyl hydrogen proceeds over a reaction barrier of 2.4 kcal mol^{-1} while the activation energy for the removal of a methyl hydrogen is a substantially higher 4.0 kcal mol^{-1}. It is interesting to note that the hydrogen with the longest C−H bond in methyl formate (the carbonyl hydrogen) is the hydrogen that is preferred for abstraction.

C. Estimation of the Rate Constant for Hydrogen Abstraction. *1. Ab Initio Rate Constant Estimation.* For reactions 1a and 1b the branching ratio is expressed as the ratio of the rate constants, i.e., k_{1d}/k_1. From simple transition-state theory each rate constant is given by the following expression:

$$k = \frac{Lk_b}{T}\frac{Q_{TS}}{Q_{OH}Q_{methylformate}}e^{E_a/RT} \qquad (6)$$

where E_a is the activation energy, T is the temperature, R is the gas constant, Q is the total partition function incorporating transnational, rotational, vibrational, and electronic partition functions ($Q_T = Q_eQ_vQ_rQ_t$), L is the statistical factor (number of equivalent carbon−hydrogen bonds), and k_b is Boltzman's constant. As mentioned, the effect of tunneling is predicted to be an important factor in evaluation of the rate constant. A one-dimensional estimate of the effect of tunneling is provided by the Wigner correction.[25] Using this correction, activation barriers for reactions 1a and 1b are calculated to be 3.0 and 1.0 kcal mol^{-1}, respectively. When these barrier heights and the partition function data listed in Table 2 are used, the rate constants for each reaction pathway are calculated. Removal of a methyl hydrogen is estimated to have a 298 K rate constant of 2.66×10^{-14} cm^3 $molecule^{-1}$ s^{-1} while removal of the carbonyl hydrogen is predicted to have a 298 K rate constant of 1.61×10^{-13} cm^3 $molecule^{-1}$ s^{-1}. The combined rate constant is thus 1.88×10^{-13} cm^3 $molecule^{-1}$ s^{-1}. Thus, 86% of the total reaction proceeds through reaction 1b, resulting in the formation of CH_3OCO radical.

TABLE 2: Energetic Parameters for Methyl Formate, Transition States, and Products

	energy[a] (G2)	thermal correction[a]	partition function[b]
OH	75.652 463	0.010 882	1.516×10^{27}
$CH_3OC(O)H$	−228.791 617	0.068 193	4.518×10^{31}
CH_3OCO	−228.120 507	0.055 184	
$CH_2OC(O)H$	−228.116 924	0.053 292	
H_2O	−76.353 640	0.024 314	
$CH_3OC(O)H$−OH	−304.437 414	0.076 289	9.633×10^{33}
HO−$CH_3OC(O)H$	−304.434 466	0.075 792	1.402×10^{34}

[a] Energies and thermal corrections in hartrees. [b] Partition functions in cm^3 $molecule^{-1}$ s^{-1}.

TABLE 3: Pseudo-First-Order Rate Constant (k') as a Function of Initial Methyl Formate Concentration

[methyl formate]$_0$ (10^{-14} molecules cm^{-3})	k' (s^{-1})	[methyl formate]$_0$ (10^{-14} molecules cm^{-3})	k' (s^{-1})
1.19	16.99	1.99	27.24
1.30	18.53	2.01	30.59
1.43	19.99	2.21	34.31
1.65	24.98	2.36	38.87
1.81	29.62		

2. Experimental Verification of the Ab Initio Rate Constant. Table 3 lists the rate constant for the reaction of methyl formate with hydroxyl radical as a function of the initial concentration

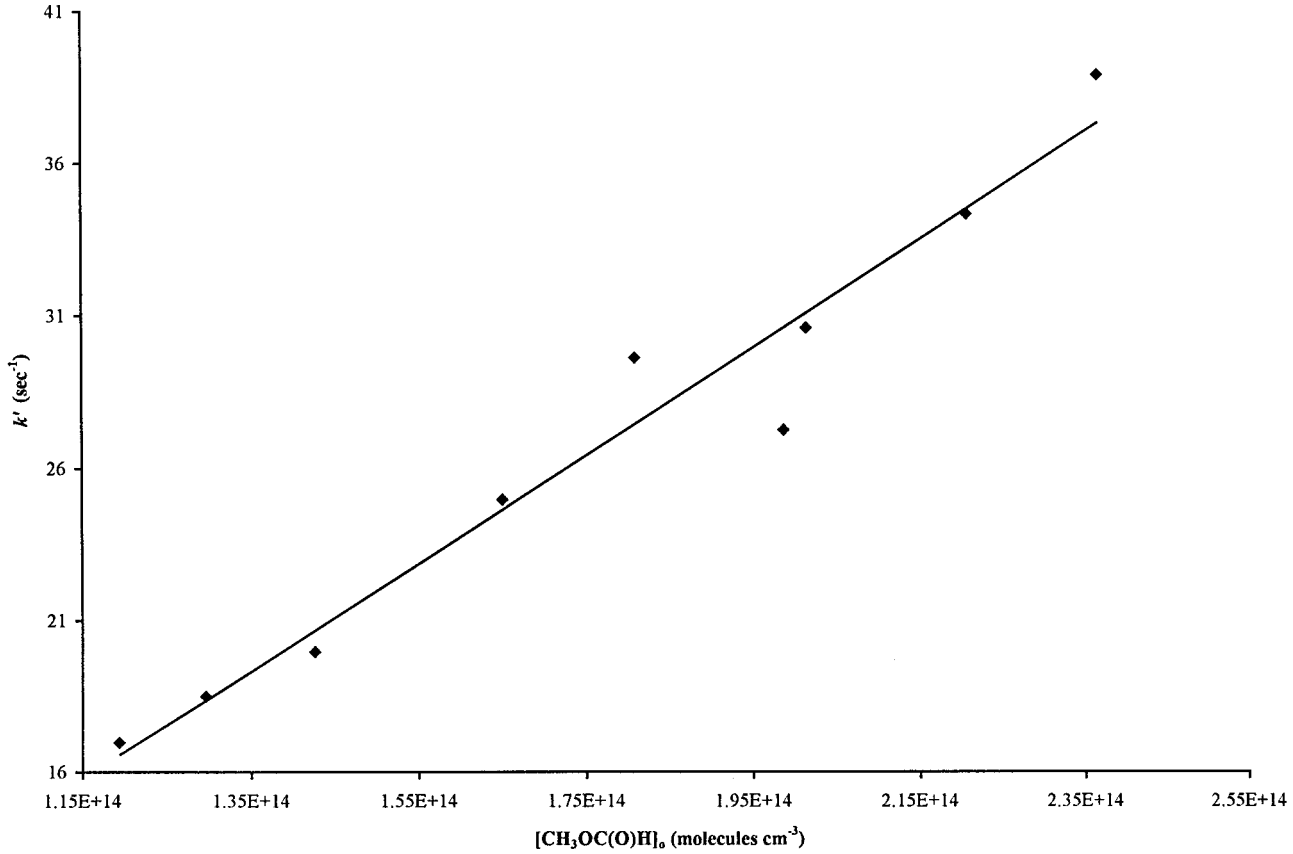

Figure 4. Pseudo-first-order decay rate of the OH radical as a function of [methyl formate]$_0$ at 298 K.

of methyl formate. Because $[CH_3OOC(O)H]_0 \gg [OH]_0$, the measurements were considered to be made under pseudo-first-order conditions. Figure 4 shows the pseudo-first-order rate constant as a function of the initial concentration of methyl formate. The slope of the fitted straight line through all data points yields a bimolecular rate constant of $(1.77 \pm 0.28) \times 10^{-13}$ cm^3 molecule^{-1} s^{-1} for the reaction of hydroxyl radical with methyl formate. Quoted errors represent two standard deviations about the least squares analysis. Our measurements are in excellent agreement with the work of Le Calve' et al.[9] and Wallington et al.[8] who report a value of $(1.73 \pm 0.21) \times 10^{-13}$ and $(2.27 \pm 0.34) \times 10^{-13}$ cm^3 molecule^{-1} s^{-1}, respectively.

D. Atmospheric Implication of Reaction 1. The results of our theoretical and experimental study of reaction 1 suggest that reaction 1b will be the dominant loss mechanism of methyl formate in the atmosphere. Under atmospheric conditions further oxidation of the CH_3OCO radical may result in the formation of carbon dioxide and formaldehyde through the following mechanism.

$$CH_3OCO \rightarrow CH_3 + CO_2 \quad (7)$$

$$CH_3OCO + O_2 \rightarrow CH_3OC(O)O_2 \quad (8)$$

$$CH_3OC(O)O_2 + NO \rightarrow CH_3OC(O)O + NO_2 \quad (9)$$

$$CH_3OC(O)O \rightarrow CH_3O + CO_2 \quad (10)$$

$$CH_3O + O_2 \rightarrow CH_2O + HO_2 \quad (11)$$

$$CH_3OC(O)O + O_2 \rightarrow CH_2O + CO_2 + HO_2 \quad (12)$$

Reactions 7 and 8 are competitive reactions for the CH_3OCO radical. The $CH_3OC(O)O$ radical resulting from reaction 8 may participate in two competing channels, reactions 10 and 12. Reaction 10 is a CO bond-cleaving reaction resulting in the formation of carbon dioxide and a methoxy radical, while reaction 12 is a hydrogen abstraction reaction mediated by molecular oxygen to form formaldehyde and carbon dioxide. The methyl radical produced in reaction 7 and the methoxy radical formed in reaction 10 undergoes further oxidation to formaldehyde. Therefore, 86% of the methyl formate may be oxidatively degraded into carbon dioxide and formaldehyde.

IV. Conclusions

The methyl formate/hydroxyl radical rate constant, as predicted by *ab initio* methodology, is estimated to be 1.85×10^{-13} cm^3 molecule^{-1} s^{-1}. This value is within the estimated uncertainties of two previous experimental determinations. Our experimentally determined rate constant of $(1.77 \pm 0.28) \times 10^{-13}$ cm^3 molecule^{-1} s^{-1} is in excellent agreement with the rate constant of $(1.73 \pm 0.21) \times 10^{-13}$ cm^3 molecule^{-1} s^{-1} determined by Le Calve' et al.,[9] which is in reasonable agreement with the rate constant determined by Wallington et al.[8] who report a 298 K rate constant of $(2.27 \pm 0.34) \times 10^{-13}$ cm^3 molecule^{-1} s^{-1}. In addition, we find that the OH radical initiated hydrogen abstraction reaction predominantly occurs (86%) at the carbonyl hydrogen of methyl formate to form the CH_3OCO radical, which may further oxidize to formaldehyde and carbon dioxide.

References and Notes

(1) Rouhi, A. M. *Chem. Eng. News* **1985**, *44*, 37.

(2) Japar, S. M.; Wallington, T. J.; Richert, J. F. O.; Ball, J. C. *Int. J. Chem. Kinet.* **1990**, *22*, 1257.

(3) Jenkin, M. E.; Hayman, G. D.; Wallington, T. J.; Hurley, M. D.; Ball, J. C.; Nielsen, O. J.; Ellerman, T. *J Phys. Chem.* **1993**, *97*, 11712.
(4) Wallington, T. J.; Hurley, M. D.; Ball, J. C.; Jenkin M. E. *Chem. Phys. Lett.* **1993**, *211*, 41.
(5) Langer, S.; Ljungstrom, E.; Ellerman, T.; Nielsen, O. J.; Sehested, J. *Chem. Phys. Lett.* **1995**, *240*, 53.
(6) Sehested, J.; Mogelberg, T.; Wallington, T. J.; Kaiser, E. W.; Nielsen, O. J. *J. Phys. Chem.* **1996**, *100*, 17218.
(7) Sehested, J.; Sehested, K.; Platz, J.; Egsgaard, H.; Nielsen, O. J. *Int. J. Chem. Kinet.* **1997**, *29*, 627.
(8) Wallington, T. J.; Dagaut, P.; Liu, R.; Kurylo, M. J. *Int. J. Chem. Kinet.* **1988**, *20*, 177.
(9) Le Calve', S.; Le Bras, G.; Mellouki, A. *J. Phys. Chem.* **1997**, *101*, 5489.
(10) Frisch, M. J.; Trucks, G. W.; Schlegel, H. B.; Gill, P. M. W.; Johnson, B. G.; Robb, M. A.; Cheeseman, J. R.; Keith, T.; Peterson, G. A.; Montgomery, J. A.; Raghavachari, K.; Al-Laham, M. A.; Zakrzewski, V. G.; Ortiz, J. V; Foresman, J. B.; Cioslowski, J.; Stefanov, B. B.; Nanayakkara, A.; Challacombe, M.; Peng, C. Y.; Ayala, P. Y.; Chen, W.; Wong, M. W.; Andres, J. L.; Replogle, E. S.; Gompeits, R.; Martin, R. L.; Fox, D. J.; Binkley, J. S.; DeFrees, D. J.; Baker, J.; Stewart, J. P.; Head-Gordon, M.; Gonzalez, C.; Pople, J. A. *Gaussian 94*, Revision D.2; Gaussian, Inc.: Pittsburgh, PA, 1995.
(11) Curtiss, L. A.; Raghavachari, K.; Trucks, G. W.; Pople, J. A. *J. Chem. Phys.* **1991**, *94*, 7221.
(12) Pople, J. A.; Head-Gordon, M.; Fox, D. J.; Raghavachari, K.; Curtiss, L. A. *J. Chem. Phys.* **1989**, *90*, 5622.
(13) Curtiss, L. A.; Raghavachari, K.; Pople, J. A. *J. Chem. Phys.* **1993**, *98*, 1293.
(14) Li, Z. *J. Phys. Chem.* **1999**, *103*, 1206.
(15) Li, Z.; Tao, Z.; Naik, V.; Good, D. A.; Hansen, J.; Jeong, G.; Francisco, J. S.; Jain, A. K.; Wuebbles, D. J. *J. Geophys. Res.* **1999**, in press.
(16) DeMore, W. B.; Sander, S. P.; Golden, D. M.; Hampson, R. F.; Kurylo, M. J.; Howard, C. J.; Ravishankara, A. R.; Kolb, C. E.; Molina, M. J. *Chemical Kinetics and Photochemical Data for Use in Stratospheric Modeling Evaluation #12*, Jet Propulsion Laboratory, Pasadena, Ca, Jan 1997.
(17) Wine, P. H; Kreutter, N. M.; Ravishankara, A. R. *J. Phys. Chem.* **1979**, *83*, 3191.
(18) Leu, M.-T. *J. Phys. Chem.* **1979**, *70*, 1662.
(19) Ravishankara, A. R.; Nlocovich, J. M.; Thompson, R. L.; Tully, F. P. *J. Phys. Chem.* **1981**, *85*, 2498.
(20) Leu, M. T.; Smith, R. H. *J. Phys. Chem.* **1981**, *85*, 2570.
(21) Leu, M. T.; Smith, R. H. *J. Phys. Chem.* **1982**, *86*, 73.
(22) Li, Z.; Freidl, R. R.; Sander, S. P. *J. Phys. Chem.* **1995**, *99*, 13445.
(23) Curl, R. E. *J. Chem. Phys.* **1959**, *30*, 1529.
(24) Pople, J. A.; Scott, A. P.; Wong, M. W.; Radom, L. *Isr. J. Chem.* **1990**, *33*, 345.
(25) Shimanouchi, T. *Tables of Molecular Vibrational Frequencies Consolidated Volume I*; National Bureau of Standards: Washington, D.C., 1972; pp 1−160.
(26) Wigner, E. P. *Z. Phys. Chem. Abstr.* **1932**, *B19*, 293.